

# Downscaling from Oceanic Global Circulation Model towards Regional and Coastal Model using spectral nudging techniques: application to the Mediterranean Sea and IBI area models

By **Herbert<sup>1</sup> G., Garreau<sup>1</sup> P., Garnier<sup>1</sup> V., Dumas<sup>1</sup> F., Cailleau<sup>2</sup> S., Chanut<sup>2</sup> J., Levier<sup>2</sup> B., Aznar<sup>3</sup> R.**

<sup>1</sup>Ifremer/DYNECO-PHYSED, Brest, France

<sup>2</sup>Mercator Ocean, Toulouse, France

<sup>3</sup>Puertos del Estado

## Abstract

In order to favour the downstream from the European MyOcean service of large scale ocean forecasts to the national service of coastal ocean forecasts, studies of new methods improving the downscaling between global or regional ocean models and coastal ones are in progress. In the framework of PREVIMER and MyOcean projects respectively, IFREMER and Mercator Ocean studied in parallel the impact of the spectral nudging method.

In the present work, the performance of spectral nudging was assessed using two regional hydrodynamic models: one of Mediterranean Sea and one of the Iberia-Biscay-Ireland (IBI) area. They are both forced by a coarser global circulation model (GCM) (PSY2V4/Mercator Ocean). This technique prevents large and unrealistic departures between the global circulation model (GCM) driving fields and the regional model fields at the GCM spatial scales.

Regarding the Med Sea application, the model's temperature  $T$  and salinity  $S$  are spectrally nudged towards PSY2V4 solution using nudging terms in the model tracer equations: a semi prognostic approach has been chosen. The simulated fields are then compared with those estimated by no-nudged model and confronted to observations. Results show that the spectral nudging is able to constrain error growth in large-scale circulation without significant damping of the meso-scales eddy fields.

Regarding the IBI application,  $T$ ,  $S$  as well as current speed  $U$ ,  $V$  have been nudged towards PSY2V4 solution: the increments are directly added as source and sink terms in the model prognostic equations. PSY2V4, nudged IBI and no-nudged IBI models as well as the present operational IBI model weekly restarted by PSY2V4 are compared and confronted to observations. The large scale and meso-scale structures are better represented off the shelf area where IBI is nudged and the bias significantly decreases on the shelf where the high frequency and high resolution physics of free IBI is better resolved than the assimilated PSY2V4 model one.

## Spectral nudging method: general description

The spectral nudging aims at forcing the regional child model solution to be close to the global parent forcing model at large scales, for which the highest quality in the forcing can be expected (thanks to data assimilation), while regional features are unconstrained. The nudging term depends on the difference of large spatial scales between the regional and global result. This term can be either positive or negative elsewhere and « nudges » the regional model solution so that it remains next to the large-scale global field. The general spectral nudging equation for a given variable  $X$  may be written as:

$$X(t+1)=X(t)+dt\{M(t)+\delta\} \text{ with } t_0 < t < t_0+T \quad (1)$$

Where  $M(t)$  is the free child model solution,  $\delta$  is the increment of  $X$  between the parent and the child models and  $T$  the assimilation window (period of the analysis cycle).

An IAU (Incremental Analysis Update, Bloom et al, 1996) process is applied for the time integration of the child model as it shown in the Fig. 1. After a forecast  $i$ -cycle of the child model, the increment  $\delta_i = \langle X_p - X_c \rangle_i$  between the parent model analysis  $X_p$  and the child model forecast  $X_c$  is calculated for a chosen state variable  $X$  (typically: the current  $U$ ,  $V$ , the temperature  $T$  and the salinity  $S$ ). The brackets " $\langle \rangle$ " consist in a time and space low pass filters which allows to take into account the only best part of the signal resolved by the parent model. A tapering function  $f(x,y,z)$ , (a spatial weight function), is applied to  $\delta_i$  in order to define where  $X_c$  has to be nudged. Then, the child system is restarted back for a 2nd  $i$ -cycle which can be called "analysis cycle". During the analysis  $i$ -cycle,  $X_c$  is nudged by  $X_p$  in following the IAU function  $g(t)$ , (a time weight function).

So, to sum up the method: after each forecast cycle of the child system, a corresponding analysis cycle is re-launched and the child system is nudged by the following final spectral nudging increment  $\delta X_{SN}$  such as:

$$\delta X_{SN} = g(t) \cdot f(x,y,z) \cdot \langle X_p - X_c \rangle = g(t) \cdot f(x,y,z) \cdot \delta$$

(2)

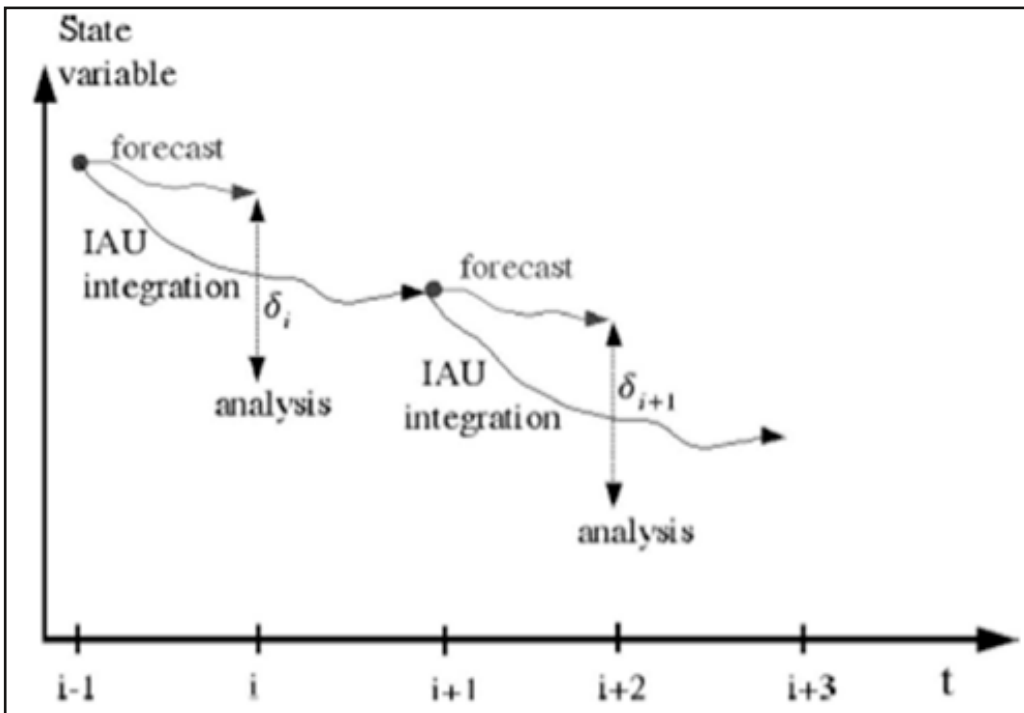


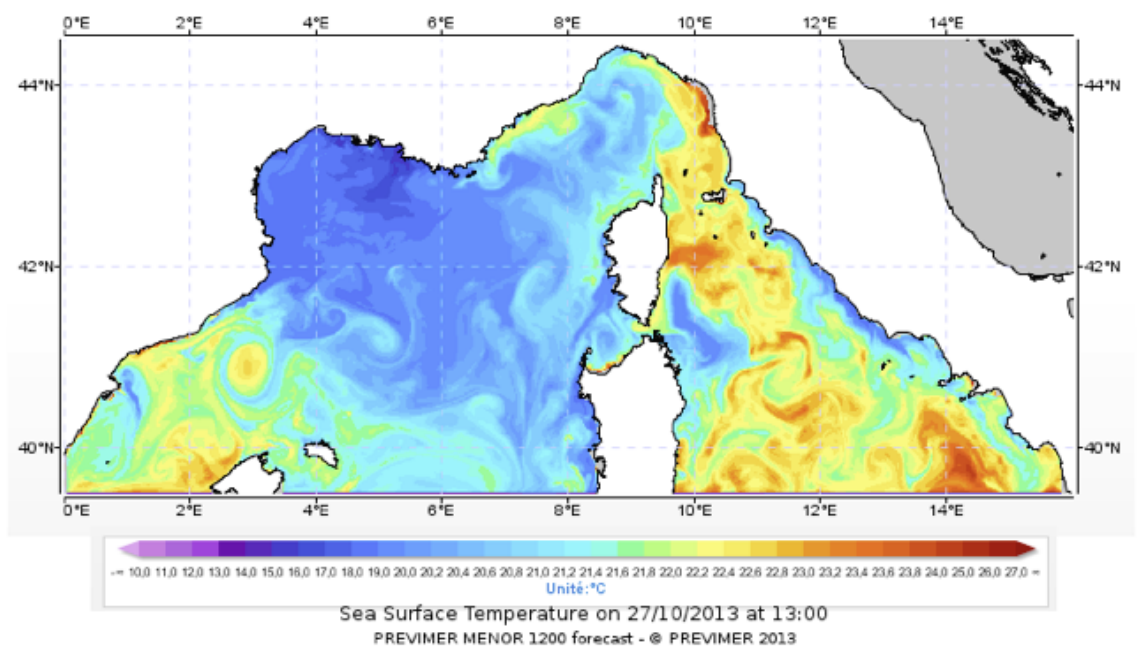
Figure 1: IAU method from Bloom et al, 1996.  $\delta_i$  is the increment of the  $i$ -cycle.

## Application to a Mediterranean Sea model

### Model configuration

The regional model used here is the MARS3D (Model for Applications at Regional Scale) developed at IFREMER, which is fully described in Lazure and Dumas (2008). The domain covers the western part of Mediterranean Sea between 39.5°N – 44.5°N and 0°E – 16°E (figure2) with a horizontal resolution of 1.2 km. There are 40 vertical levels, formulated using generalised sigma coordinate system. The open boundaries and initial conditions are provided by the global solution from Mercator Ocean (PSY2V4), at a horizontal resolution of 6 km, which is assimilated with SLA, SST and (T, S) profiles. The global solution is prescribed along the southern open boundary conditions without any nudging within the domain's body. The atmospheric forcing was specified according to the ALADIN (Aire Limitée Adaptation dynamique Développement InterNational) model from Météo-France. The fields were provided with a time resolution of 3 hours. This configuration is similar to the MENOR configuration proposed by PREVIMER for the regional Mediterranean forecast. Additional details about the MARS3D numerical code can be found in previous papers (<http://www.ifremer.fr/mars3d/References/Publications>).

Figure2: Domain of interest.



## Downscaling from Oceanic Global Circulation Model towards Regional and Coastal Model using spectral nudging techniques: application to the Mediterranean Sea and IBI area models

### Experiments

The specific spectral nudging method chosen to nudge this Med Sea model is based on the semi-prognostic method described by Eden and al. (2004) and revisited by Sheng and al. (2005). The authors achieved the implementation by adding nudging terms to part of the model equations such as motions equation (nudge on density gradient term) or thermodynamic equation (nudge on temperature and salinity) (von Storch et al. 2000; Alexandru et al. 2009). In our case, the spectral nudging was applied only for temperature and salinity. The spatial filter used here is a 2D convolution filter, which spatially smooths the misfits between global and regional model in temperature and salinity and filters out the wavelengths smaller than a cut-off scale. Regarding the time integration function  $g(t)$ , the increment  $\delta$ , which acts as an external forcing, is time constant over the temporal window  $t$ . In the present analysis, the spectral nudging increments are built over a period of  $t=7$  days and spatially filtered over a window of 50 km. Regarding the tapering function  $f(x,y,z)$ , the nudging was set to zero for water depths smaller than 500 m, so that the regional processes on the shelf are not affected, and a nudging coefficient  $\alpha$  can be defined.

The year 2010 has been chosen for the practical numerical experiences. The first simulation is a free run (i.e. without spectral nudging), leaving its temperature and salinity fields free to evolve all along the year. It is considered as the reference simulation, according to which the efficiency of the assimilation method will be assessed. The different steps of the 'nudged run' are depicted on the flow chart on figure 3: MARS3D is first freely run over a time-window, which determines the frequency bands selected for the increment. The difference of the regional/global temperature and salinity fields averaged over this time-window is computed from the global model fields interpolated on the regional model grids. The field of the differences is then spatially filtered out through a 2D convolution filter. This nudging term is finally introduced in temperature and salinity transport equation of the regional model as a constant sink or source term. The controlled solution of the regional model is then integrated over 7-days time-window. We repeat this from time to time over the year 2010. The effect of spectral nudging on the realism of the numerical solutions is afterwards evaluated by comparison with satellites and in-situ observations.

The main characteristics of the free simulation and the nudged simulation are listed in table 1.

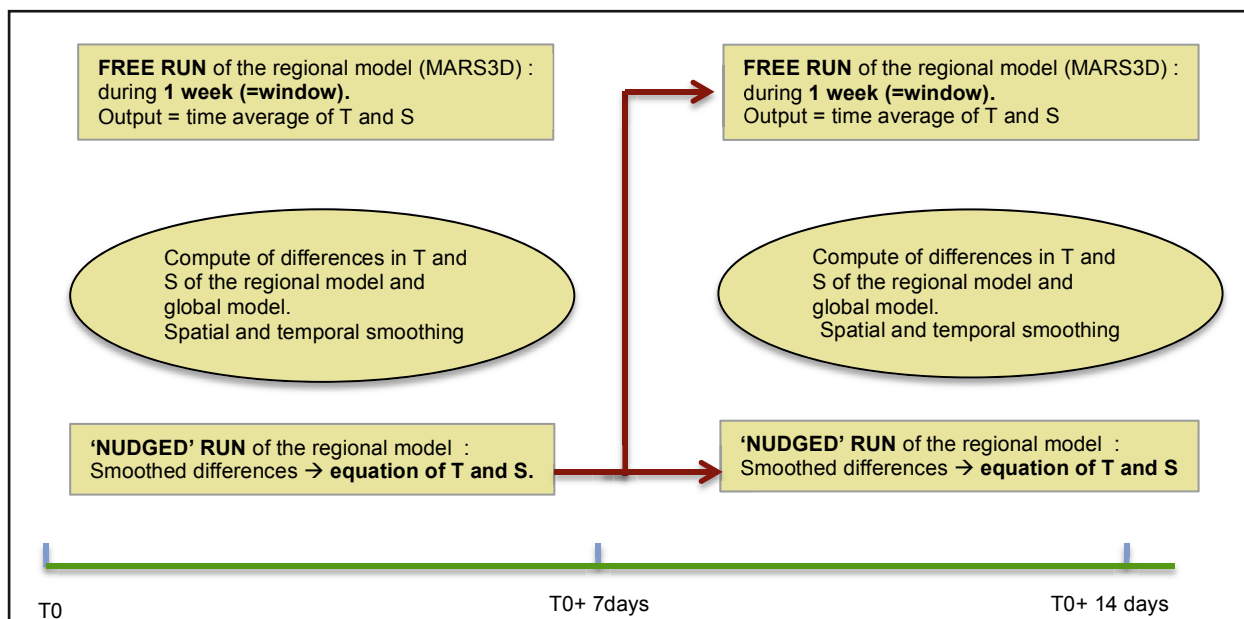


Figure 3 : Diagram presenting the spectral nudging method in temperature and salinity applied to the regional model MARS3D. February 2014 at 15:15

Simulation ID	Spectral nudging	Time window	Nudging coefficient $\alpha$	Nudging Applying	Spatial window
1- Nudged run	Yes	7 days	1/7.5	Bottom > 500 m	50 km
2- Free run	No	----	----	----	----

Table 1: Nudging parameters applied to the 'nudged simulation' (with applying of spectral nudging), in contrast with the 'free simulation' (i.e. without applying of spectral nudging).

**Results - Discussion**

**Comparison with SST from SEVIRI data.**

In order to determine how the assimilation method impacts the sea surface temperature, we compare SST data from SEVIRI to simulated SST from the regional model, with and without spectral nudging applied over the year 2010. Figure 4 shows the time series of the spatial average of SST over the year 2010 of the nudged solution, the free simulation and from the global model PSY2V4, as well as the root mean square errors (RMSE) of each.

Although the free simulation captures rather correctly the basic SST evolution, we notice a negative bias compared to the SEVIRI data from July to September. Indeed, the RMSE during this period reach 2.8°C whereas they are ranged from about 0.5 to 1.5°C the rest of the time (see table 2). The match is better for the global simulation where the RMSE does not exceed 1.5 °C in summer in agreement with the fact that the global solution is an analysis including SST observations. The use of spectral nudging reduces noticeably the biases and the RMSE and succeeds in maintaining the regional model next to the global analysis. On the contrary, in June and August, it performs less efficiently and even hardly improves the regional solution whatever the quality of the global analysis: the RMSE in August is slightly increased from 1.17 °C (free run) to 1.22 °C (the nudged run). It might be due to a link between this observed bias and the small scales activity.

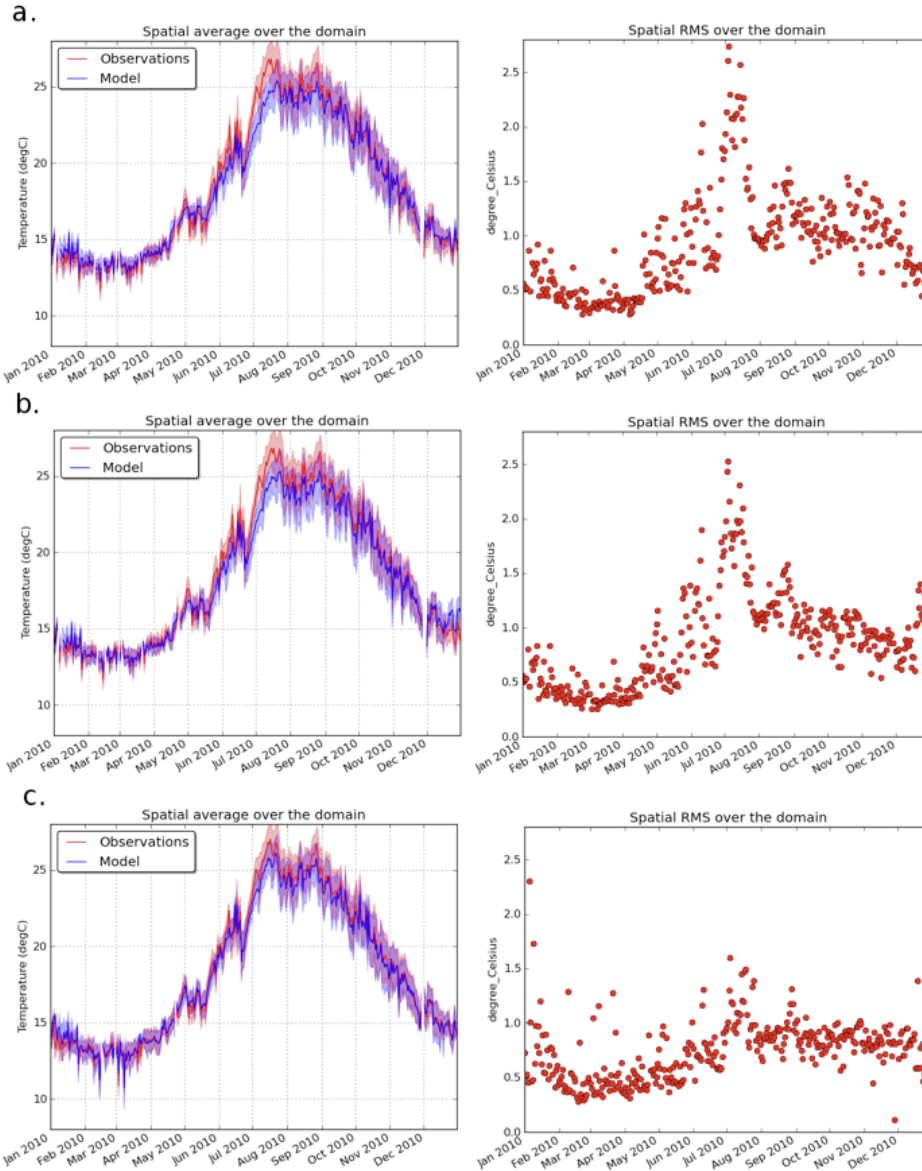


Figure 4 : Observed (red line) and simulated (blue line) daily sea surface temperature (°C) (left panel), and spatial rms over the domain (right panel) from the free simulation (a), the nudged simulation (b), and the global model PSY2V4 (c), over the year 2010. Observed daily SST data are provided by Spinning Enhanced Visible and InfraRed Imager (SEVIRI).

Table 2: Monthly rms errors between observed and simulated SST (in °C) provided by the nudged simulation, the free simulation and the global model PSY2V4 over the year 2010.

Month	Nudged run	Free run	PSY2V4
Janv.	0.54	0.60	0.61
Feb.	0.39	0.42	0.43
Mar.	0.36	0.40	0.48
Apr.	0.51	0.51	0.47
May	0.75	0.81	0.60
Jun.	1.10	1.14	0.73
Jul.	1.69	1.77	1.09
Aug.	1.22	1.17	0.91
Sep.	1.00	1.09	0.83
Oct.	0.98	1.10	0.87
Nov.	0.86	1.08	0.77
Dec.	0.98	0.74	0.71

## Downscaling from Oceanic Global Circulation Model towards Regional and Coastal Model using spectral nudging techniques: application to the Mediterranean Sea and IBI area models

Figure 5 shows an example of mean SST over November 2010 from SEVIRI observations, from the free regional model and from the nudged model, as well as the monthly mean bias (difference between observation and model field) associated. The results show that the regional model driven only at its lateral boundaries presented a warm bias in the middle of the domain (at the east of Baleares islands and at the north-west of Corsica). These biases that may reach  $-4^{\circ}\text{C}$  are largely reduced thanks to the nudging. However, some biases remain. Some of them are also present in the global model, as the warm bias observed at the east of Corsica. These cold waters result in intense mixing induced by strong westerly winds channelled between Corsica and Sardinia. They are clearly visible on satellite observations but missing in regional and global model. The nudging of the regional solution towards global solution will have a negative effect in this case. Other biases are specific to regional model dynamic, as the cold bias associated to river discharge (the « Rhone », at the east coast of Gulf of Lions, and the « Ebre », at Spanish coast), visible in the free simulation and maintained in nudged simulation since the spectral nudging is not applied on the shelf. These too cold waters has the effect the destruction of the warm surface signature associated to the North Current (i.e. Liguro-Provençal Current), which goes along the coast along the  $\sim 200\text{m}$  isobath and which is well visible in satellite observation and in the global simulation field.

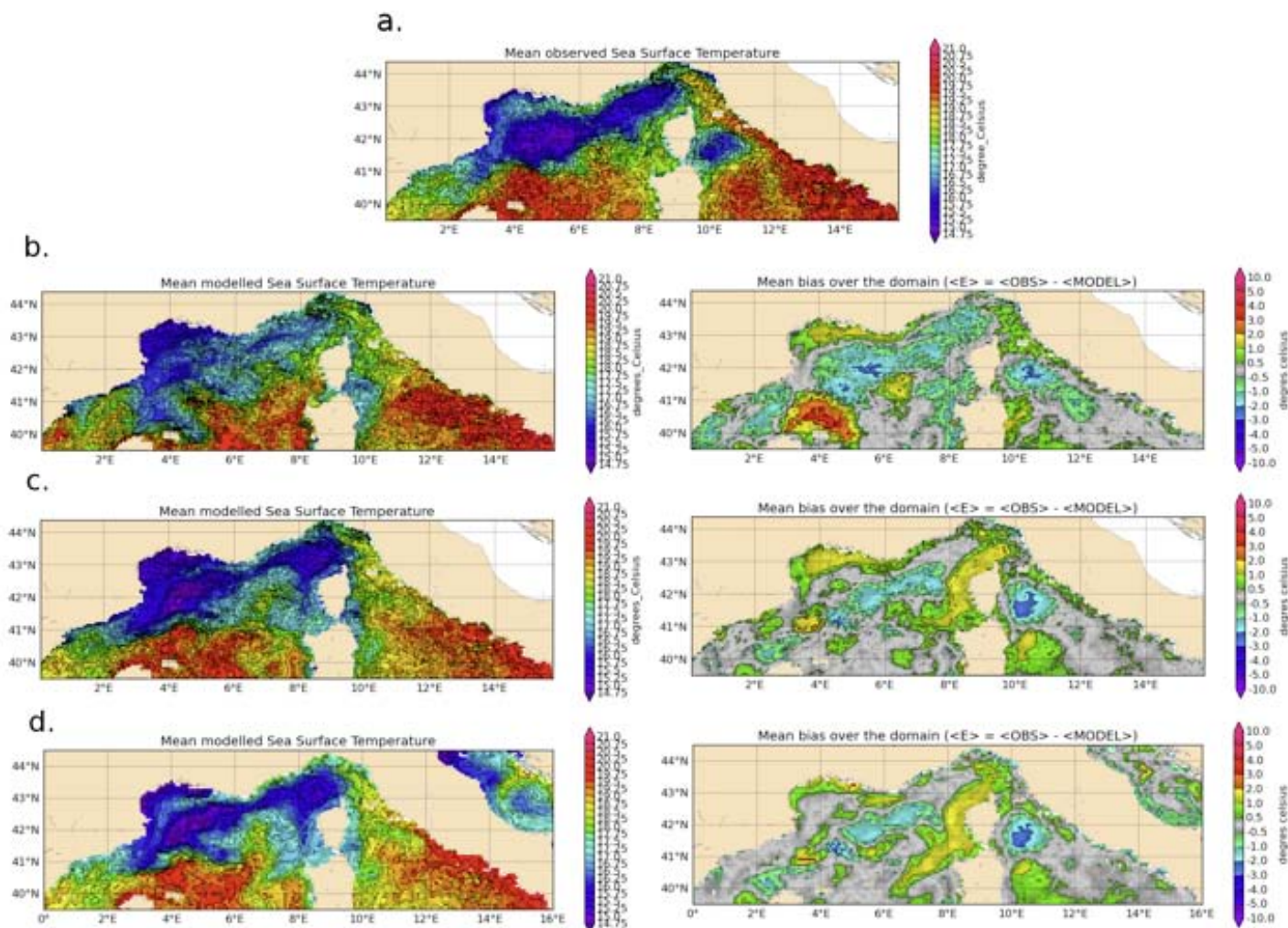


Figure 5 : SST ( $^{\circ}\text{C}$ ) over November month 2010 from SEVIRI satellite data (a), the free simulation (b), the nudged simulation (c), the global model PYS2V4 (d), and the mean bias (observation-model) associated.

### Modelling of Levantine water.

The Levantine Intermediate Water (LIW) is an important water mass for the overall hydrology and processes of the north-western of the Mediterranean Sea. They are formed in the Levantine Basin (easternmost Mediterranean area) during winter (Wüst, 1961; Lascaratos et al., 1993) and are characterised by a subsurface maximum of salinity (ranging from 39.0 psu in the Levantine basin to 38.5 psu in the Western Mediterranean), separating deep water from surface waters. One part contributes to the Liguro-Provençal Current (LPC) along French and Spanish coast, which is one of dominant process of the coastal dynamic of North Mediterranean region. The second part spreads in the whole areas at a depth ranging from 400 to 600 m. A realistic representation of these waters is essential in order to get a correct dynamic over the north-western basin, particularly the dense water formation during winter (MEDOC group, 1970, Millot, 1987, 1990, 1999, etc). The analysis of the volume of this water mass over 2010 is conducted in order to estimate the realism of each model and the efficiency of the spectral nudging with respect of the LIW preserving ability. Figure 6 shows a vertical section of salinity characteristic of LIW (i.e. ranged between 38.48 psu and 38.86 psu) along the latitude  $42^{\circ}\text{N}$  on January 15<sup>th</sup> 2010 (i.e. 15 days after the start of the simulation) and on December 11<sup>th</sup> 2010, from the PSY2V4 model, and from the regional model MARS3D without and with applying of spectral nudging.

Downscaling from Oceanic Global Circulation Model towards Regional and Coastal Model using spectral nudging techniques: application to the Mediterranean Sea and IBI area models

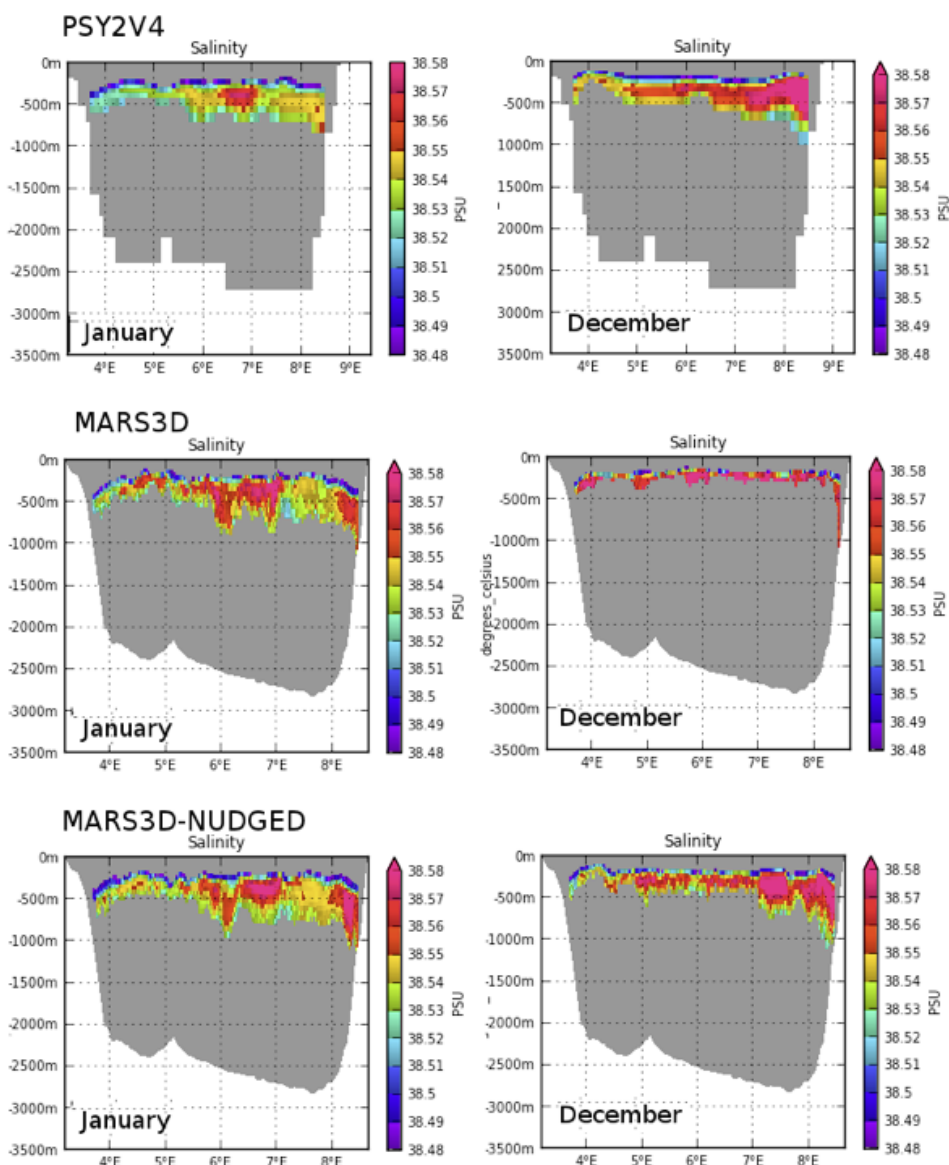
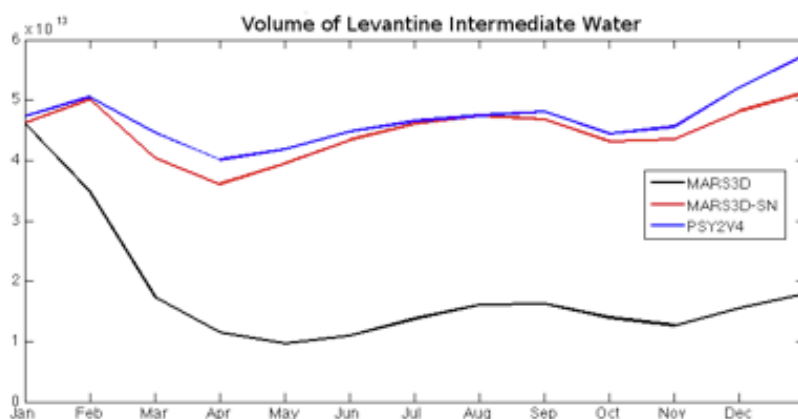


Figure 6: Vertical section of the salinity (psu) at the latitude 42°N on January 15th 2010 (left panel) and on December 11th 2010 (right panel), from the global model PSY2V4, and the regional model MARS3D without and with using of spectral nudging technique. Only the temperature ranged between 13.2°C and 14.2°C, the salinity ranged between 38.48 psu and 38.88 psu, and the depths 300m to 600m, characteristics of Levantine waters, are shown.

It can be seen in the global analysis PSY2V4 that the LIW extends from the Ligurian Sea to the Liguro-Provencal basin, between 300 m to 600 m depths. In January, the LIW represent 11% of the total volume of water masses (figure 7). The volume of LIW introduced into the basin fluctuates over months between a minimum on April (around  $4.10 \cdot 10^{13} \text{ m}^3$ ) and a maximum of  $5.8 \cdot 10^{13} \text{ m}^3$  at the end of the year. The restoration of LIW volume is not correctly represented by the regional model MARS3D (figure 6 right panel). Indeed, results show that the volume of LIW in December is not as high that in January: the volume of LIW decreases from  $4.6 \cdot 10^{13} \text{ m}^3$  (i.e. 11% of the total volume of water masses) at the start of the simulation (January 2010) to  $1.8 \cdot 10^{13} \text{ m}^3$  (i.e. 4% of the volume total of water masses) at the end of the simulation (December 2010) (figure 7). This water mass, which percentage could be considered as weak, plays an essential role in the constitution of dense and deep water in north-eastern Mediterranean Sea. A good control of these waters allows maintaining a realist cyclonic circulation in the northern part of the basin. The spectral nudging by putting the regional solution on the tracks of the global analysis allows to improve the seasonal variations of the LIW (see figure 6 and figure 7). This result is confirmed by the time evolution of the LIW's volume shown in figure 7: the variations of the volume of LIW over 2010 from the nudged simulation (red curve) are of an order of magnitude very close as the global model ones (blue curve) with values ranged from  $3.6 \cdot 10^{13} \text{ m}^3$  to  $5.2 \cdot 10^{13} \text{ m}^3$ .

Figure 7: Time evolution (one value every 30 days) of the volume of Levantine Intermediate Water (in  $\text{m}^3$ ) over the year 2010 from the free simulation MARS3D, the nudged simulation (noted 'MARS3D-SN') and the global model PSY2V4.



## Downscaling from Oceanic Global Circulation Model towards Regional and Coastal Model using spectral nudging techniques: application to the Mediterranean Sea and IBI area models

### Impact on mesoscale eddy field

In this section we assess the effect of the procedure on small scale features. A spectral analysis of the kinetic energy over a rectangular domain is performed (figure 8). The monthly mean SSH spectrum over February for the free simulation, the nudged simulation and from the global analysis give an idea of the 'effective resolution' of each model. It corresponds to the smallest small scales correctly resolved by the model and for which the dissipation terms in space and time become active (Skamarock, 2004). It is defined by the wavelength from which the spectrum of the model deviates to the slope of the energy cascade. The SSH spectrum of both simulations follow approximately the  $k^{-5/3}$  slope (dashed line on the figure 8) for the large scale (wavelengths > 100km) and the  $k^{-4}$  slope (blue line on the figure 8) for the mesoscale range, in agreement with recent development in very high resolution model (Klein, 2008). For the free model, the energy cascade leaves the  $k^{-4}$  slope for wavenumber of 0.09 cycles/km indicating an effective resolution of around 11 km. In the same way, we obtain an effective resolution of 45 km for the global model.

As far as the nudged model is concerned, the spectrum tends to follow the global model one for the large scales (wavelength > 100 km) and the free model for the smallest scales, with a similar effective resolution. We notice that the energy associated to scales smaller than 50 km is not significantly reduced by the nudging process; the spectrum of the nudged model exhibits a similar spectral slope behaviour to the SSH  $k^{-4}$  slope, just as the free model. This results are confirmed on the figure 9 which presents the time evolution over 2010 of the energy associated to wavenumbers lower than 0.01 cycles/km, (i.e. wavelength > 100 km) (figure 9.a), and to wavenumbers ranging between 0.02 cycles/km and 0.03 cycles/km (i.e. wavelength between 33 km and 50 km) (figure 9.b), for the free model (blue line) and for the nudged model (red line). The time series of energy associated to scales higher than 100 km from the nudged model tends to follow the global model one whereas the time series of energy associated to scales ranging between 33 km and 50 km tends to follow the free model one.

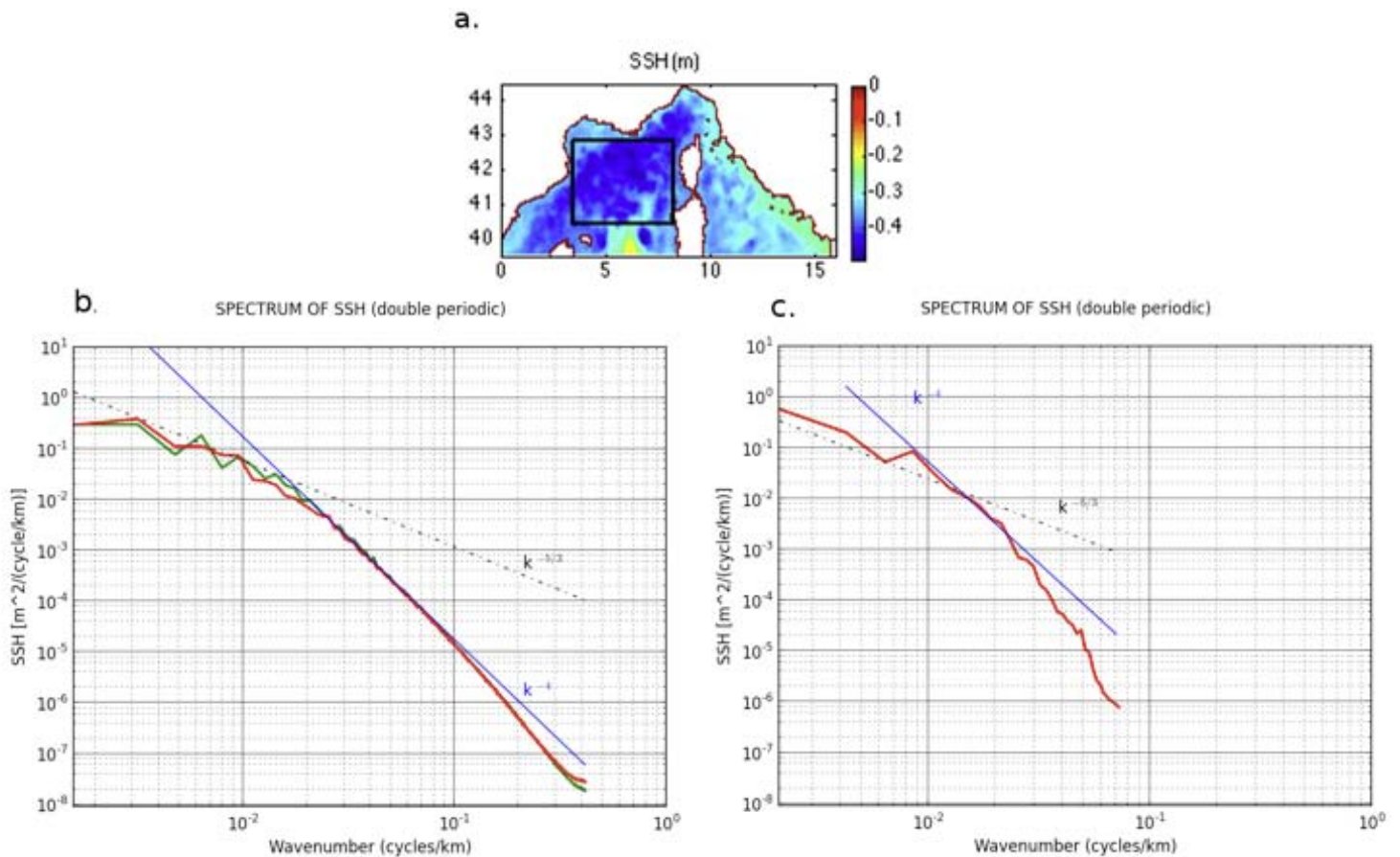


Figure 8: SSH spectrum mean over February month, from the free simulation (b; green curve), the nudged simulation (b; red curve), and the global model PSY2V4 (c). The lines indicate the  $-5/3$  (dashed) and  $-4$  (solid) slopes. The area on which the SSH spectrum has been computed is indicated by the black square on a) (the color field represents the SSH (m) on Feb.15th)

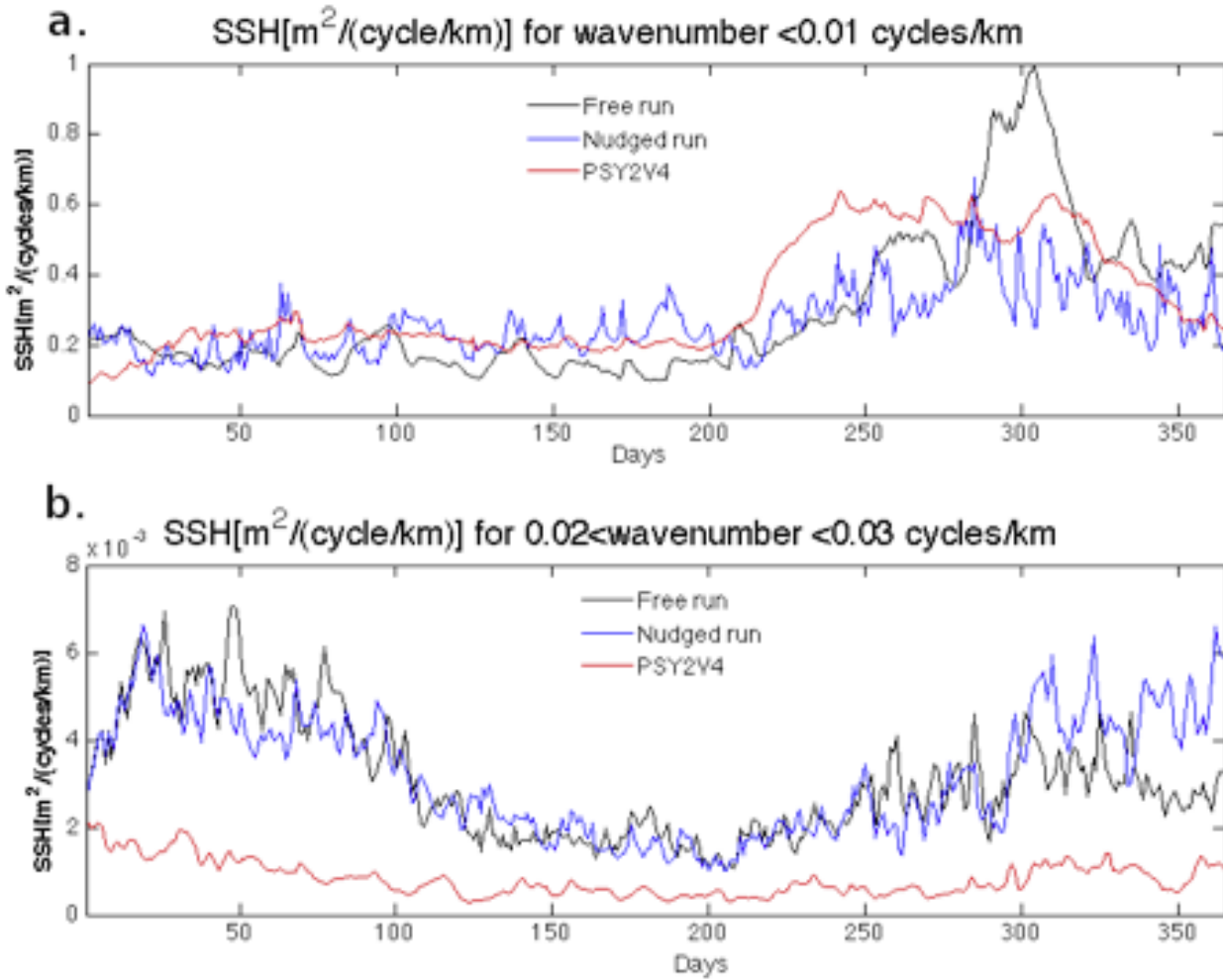


Figure 9: Time series of SSH energy associated to wavenumber a)  $< 0.01$  cycles/km and b) ranging between 0.02 cycles/km to 0.03 cycles/km (i.e. wavelength between 33 km to 50 km) over the year 2010, from the free simulation (black curve), the nudged simulation (blue curve) and the global model PSY2V4 (red curve).

The kinetic energy over the domain, representative of the mean and mesoscale activity, is computed from geostrophic velocities deduced from sea surface height. The results obtained for March 2010 are presented on figure 10 and 11, which shows the monthly mean Total Kinetic Energy (TKE), the Mean Kinetic Energy (MKE) and the Eddy Kinetic Energy (EKE), from the simulations MARS3D with and without spectral nudging and from the global model. The Total Kinetic Energy is the time averaged kinetic energy. It is calculated as:

$$TKE = \frac{1}{2} (u_g^2 + v_g^2) \quad (3)$$

Where  $u_g$  and  $v_g$  are respectively the zonal and meridian component of geostrophic velocities, calculated as follows :

$$u_g = -\frac{g}{f} \frac{\partial \eta}{\partial x} \quad \text{and} \quad v_g = -\frac{g}{f} \frac{\partial \eta}{\partial y} \quad (4)$$

With  $\partial \eta$  the slope of sea level anomaly. The Mean Kinetic Energy is computed from the time-averaged velocities, and the Eddy Kinetic Energy is the difference between the TKE and the MKE. From both simulations, high EKE is associated with the variability of the along slope Liguro-Provencal Current. EKE values are of the order of 100 cm<sup>2</sup>/s<sup>2</sup> in the regional simulations and around 40 cm<sup>2</sup>/s<sup>2</sup> in the global one. Another region of high intensity (locally  $> 90$  cm<sup>2</sup>/s<sup>2</sup> in the regional simulation), at the west of Sardinia corresponds to the Balearic front well-known for its mesoscale activity. As expected, this region is much less energetic in the global model. In the regional model, some patches of activity (around 70 cm<sup>2</sup>/s<sup>2</sup>) are found in many places in the whole basin due to the occurrence of sporadic and recurrent eddies or gyres (such as Bonifacio Gyres). The lowest energies ( $< 50$  cm<sup>2</sup>/s<sup>2</sup>) are observed in the Liguro-Provencal basin and in the Tyrrhenian Sea.

## Downscaling from Oceanic Global Circulation Model towards Regional and Coastal Model using spectral nudging techniques: application to the Mediterranean Sea and IBI area models

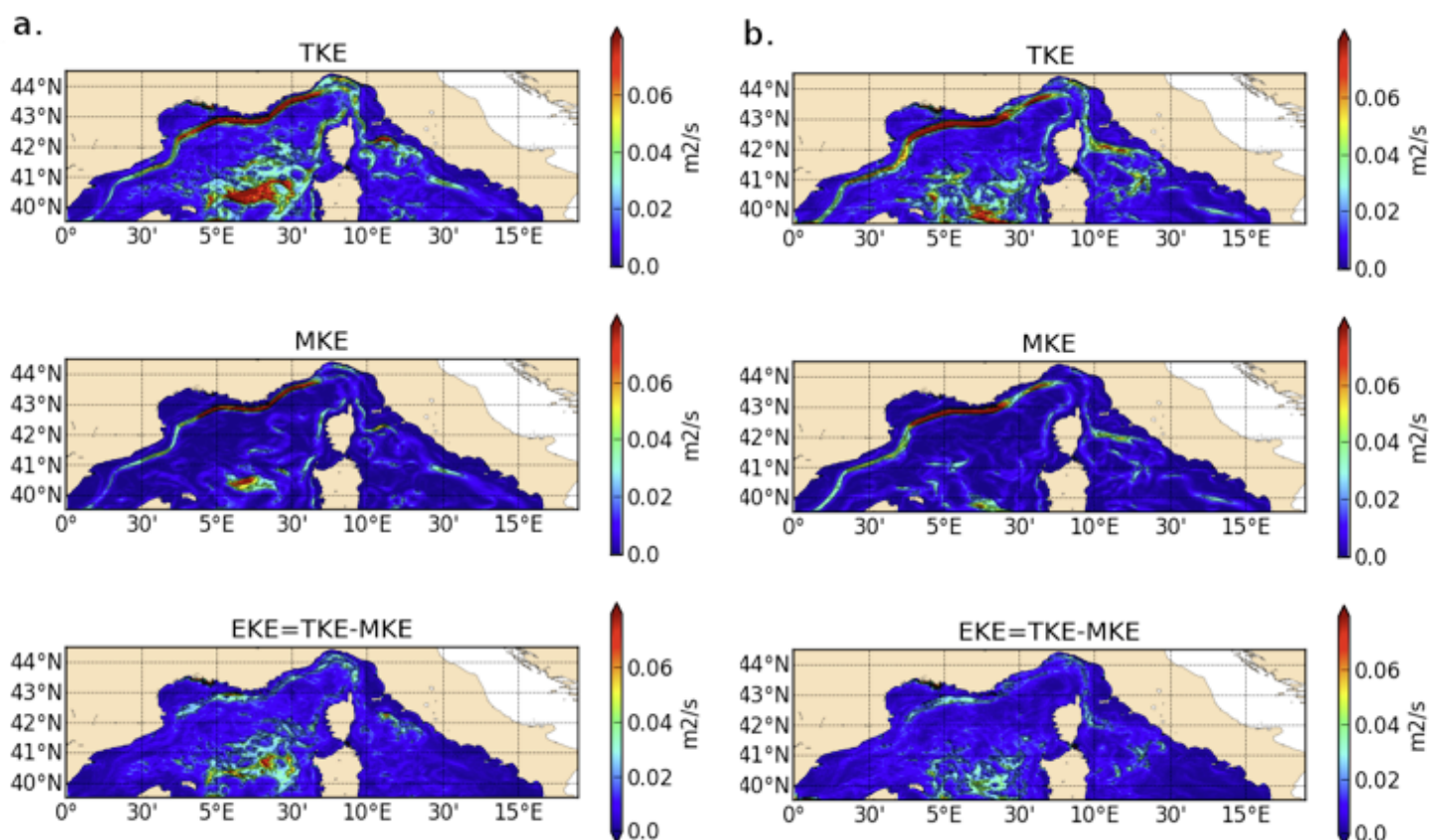


Figure 10: Mean of Total Kinetic Energy (TKE), Mean Kinetic Energy (MKE) and Eddy Kinetic Energy (EKE) in  $m^2.s^{-1}$  over March 2010, from the free simulation (a) and from the nudged simulation (b).

The spatial distribution of high and low patches of EKE is similar from both (free and nudged) simulations: slightly smaller values are present in the nudged simulation than in the free simulation, especially at the south of the domain, in the area of eddies formation. The reduction in the whole of the domain is not significant: -4.5% of the spatial average of TKE. Thus, the smallest scales, which were not driven by the spectral nudging, were not significantly affected by scale interaction.

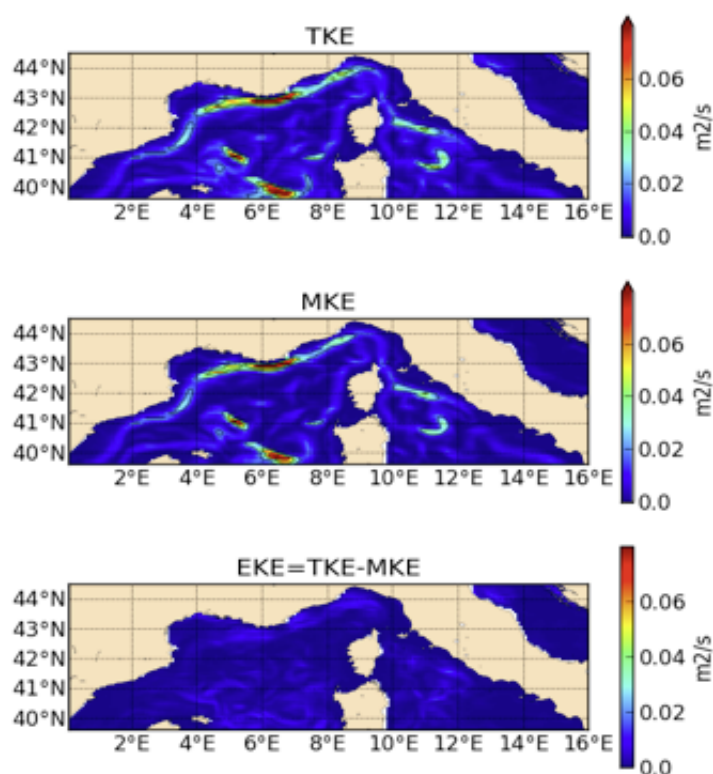


Figure 11: Same as figure 8 but from the global model PSY2V4.

## Application to an Iberia-Biscay-Ireland area (IBI) model

### Model configuration

The regional model used here is based on NEMO code (Madec et al., 1998; Madec, 2008). The model domain covers part of the North East Atlantic ocean, going from the Canary Islands to Iceland. It encompasses also part of the Western Mediterranean Sea and the North Sea, reaching to the Skagerrak Strait that connects the Baltic Sea to the North Sea. The primitive equations are discretized on a  $1/36^\circ$  ( $\sim 2$  km) curvilinear ORCA grid and on 50 z-levels in the vertical. Vertical resolution decreases from  $\sim 1$  m near the surface to more than 400 m in the abyssal plain. The open boundaries and initial conditions are provided by the global solution from Mercator Ocean PSY2V4 system. The global solution is prescribed along the open boundary conditions without any nudging. The atmospheric forcing was specified according to the 3-hourly. This configuration is similar to the configuration of MyOcean operational IBI system which runs in nominal mode at Puertos Del Estado and in backup mode at Mercator Ocean. Additional details about IBI system, its configuration description and its assessment can be found in Maraldi et al. 2013, Cailleau et al. 2012.

### Experiments

In this case, the spectral nudging is applied for  $T$  and  $S$  as well as the current speed components  $U$ ,  $V$ . As the large scale parent system PSY2V4 is supposed to resolve the meso-scale structures (up to the mid-latitudes at least) and as the representation of these structures in term of geostrophic turbulence are improved by the data assimilation of the sea level anomalies among other, IBI system must be nudged by the PSY2V4 resolved scales from large scale to meso-scale. So the space and time filters have been chosen in order to keep these scales and remove the smaller ones. Regarding the time filter, as the week is the typical characteristic time scale of the meso-scale structures, the chosen time smoothing consists in a simple weekly mean of  $X_p - X_c$ . Regarding the space filter, the spectral analysis allows to define the energy injection scale of a system ie. The wave length where the energy spectrum of the system leaves the slope of the energy cascade, and the system starts to become dissipative. In theory, the large scale follows the  $k^{-5/3}$  power law and the mesoscale follows the  $k^{-3}$  power law (see in Fig. 12). Finally, the energy injection scale could be defined as the effective resolution of a system, and can be used as the cutoff length  $T_c$  for the space low pass filter. So the parent system is able to resolve structures from the large scale to the energy injection scale. As it is presented in Fig. 12, a preliminary study has shown that  $T_c \sim 7\Delta x \sim 45$  Km can be chosen for PSY2V4 in mid latitude, between  $30^\circ$  and  $40^\circ$ N, (with  $\Delta x = 1/12^\circ$  the horizontal resolution of PSY2V4).

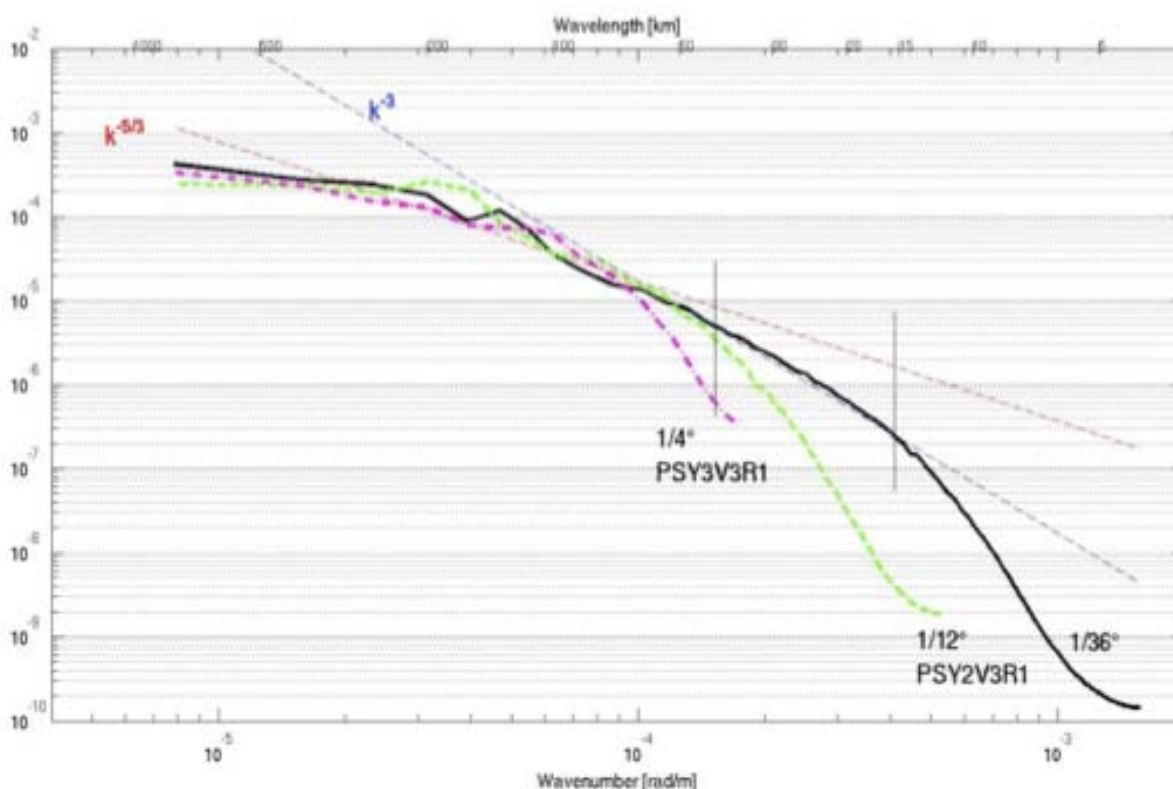
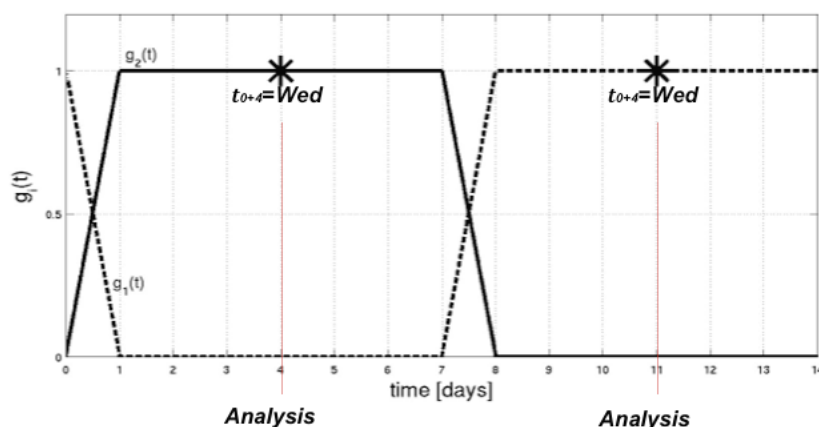


Figure 12: Spectral analysis of the large scale  $1/4^\circ$  system PSY3 (dotted and dashed pink spectrum), the eddy resolving/permitting  $1/12^\circ$  system PSY2 (dashed green spectrum) and the high resolution regional  $1/36^\circ$  IBI system (solid black spectrum). For each system, this spectra has been calculated off the Iberian coast  $s$  between about  $30^\circ$  and  $40^\circ$ N of latitude. The red dashed line corresponds to the energy cascade of the large scale and the blue one corresponds to the mesoscale energy cascade. The vertical solid black lines indicate the energy injection scale of PSY2 and IBI which is  $7\Delta x$  here (with  $\Delta x$  = horizontal resolution of each system).

## Downscaling from Oceanic Global Circulation Model towards Regional and Coastal Model using spectral nudging techniques: application to the Mediterranean Sea and IBI area models

During the analysis cycle of  $t=7$  days, the increment  $\delta$  is applied to the IBI model at each time step, by following the IAU function  $g(t)$  shown in Fig. 13. In order to prevent a discontinuity between the increments  $\delta_{i-1}$  and  $\delta_i$  of two successive analysis cycles  $i-1$  and  $i$  and so to ensure the transition between two cycles, a 1-day overlap is applied which corresponds to the linear decrease in the weight on  $\delta_{i-1}$  and the linear increase in the weight on  $\delta_i$ . The nudging was applied off the shelf (for the bottom depth  $> 200\text{m}$ ), off the coasts (from  $30\text{Km}$ ) and above depths from  $3000\text{m}$ .

Figure 13: Mercator IAU function  $g(t)$



We simulated the period from 2010/03/30 to 2010/10/18 with and without spectral nudging. So as the previous study in Med Sea, we launched a free run IBI-REF as a reference and a nudged run IBI-NUDG. The impact of the spectral nudging has been assessed by comparing the results of IBI-REF, IBI-NUDG, PSY2V4 as well as the present operational IBI system (called here IBI-OPER). The comparison with satellites and in-situ observations has been also done.

The main characteristics of the free simulation and the nudged simulation are listed in table 3.

Simulation ID	Spectral nudging	Time window	Nudging Applying	Spatial window
1- Nudged run IBI-NUDG	Yes	7 days	1- Bottom $> 200$ m 2- 30km off coast 3- Depth $> 3000\text{m}$	45 km
2- Free run IBI-REF	No	----	----	----

Table 3: Nudging parameters applied to the 'nudged IBI simulation' (with applying of spectral nudging), in contrast with the 'free IBI simulation' (i.e. without applying of spectral nudging).

## Results - Discussion

We have assessed the chosen spectral nudging method by comparing the free simulation IBI-REF, the simulation IBI-NUDG nudged by PSY2V4 off the coasts and shelf, the PSY2V4 simulation and the operational simulation IBI-OPER which is restarted every weeks with a 2-week spin up. The solutions are compared to observations. One of the main objectives of this work is to study whether IBI-NUDG solution is better than IBI-OPER, in which case we could then apply the spectral nudging method to the next IBI operational version.

IBI-OPER is able to keep track the large scale baroclinic patterns of the PSY2V4 system, and therefore, take benefit from the assimilation used on the large scale. But this simple restarting method has 2 significant drawbacks: (i) the time discontinuity inherent to the periodic re-initialization and (ii) the dependency to the large scale system on the shelf where water properties are largely biased by the missing physics. Thus, the solution of IBI-OPER is strongly constrained by the global one. But contrary to the large system, the IBI model configuration allows to resolve regional physical processes by taking into account higher frequency signals (such as tide, diurnal cycle ...) and their nonlinear interactions with the low-frequency circulation. Also the coastline, coastal bathymetry and coastal forcings (runoff) are better represented in the regional system. So the solution IBI-REF is better in the shelf area where most of high frequency processes occur. The spectral nudging method chosen for IBI-NUDG has permitted to "nudge" the low frequency IBI system solution towards the large scale PSY2V4 solution where this one is supposed to be better (off the shelf) and has permitted to let free the IBI solution on the shelf where the regional model physics is better adapted.

The IBI-REF, PSY2V4 and IBI-NUDG daily mean Sea Level Anomaly (SLA) has been qualitatively compared to AVISO one off the Gibraltar straight. In Fig. 14, the date of 2010-09-16 is taken as an example. PSY2V4 solution is obviously coarser than IBI-REF one but the meso-scale structures are better positioned due to the SLA assimilation. In this area, IBI-NUDG solution is closer to the AVISO SLA than IBI-REF by taking benefit of PSY2V4 solution with a best resolution of eddies and SLA gradients.

Downscaling from Oceanic Global Circulation Model towards Regional and Coastal Model using spectral nudging techniques: application to the Mediterranean Sea and IBI area models

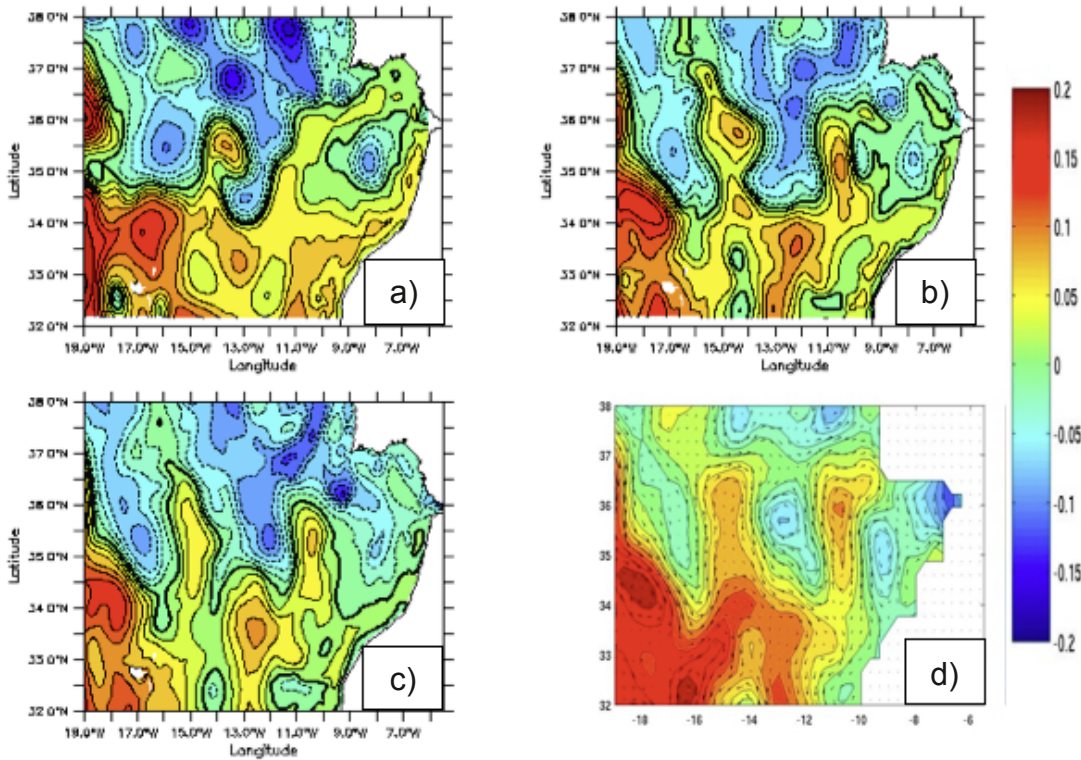
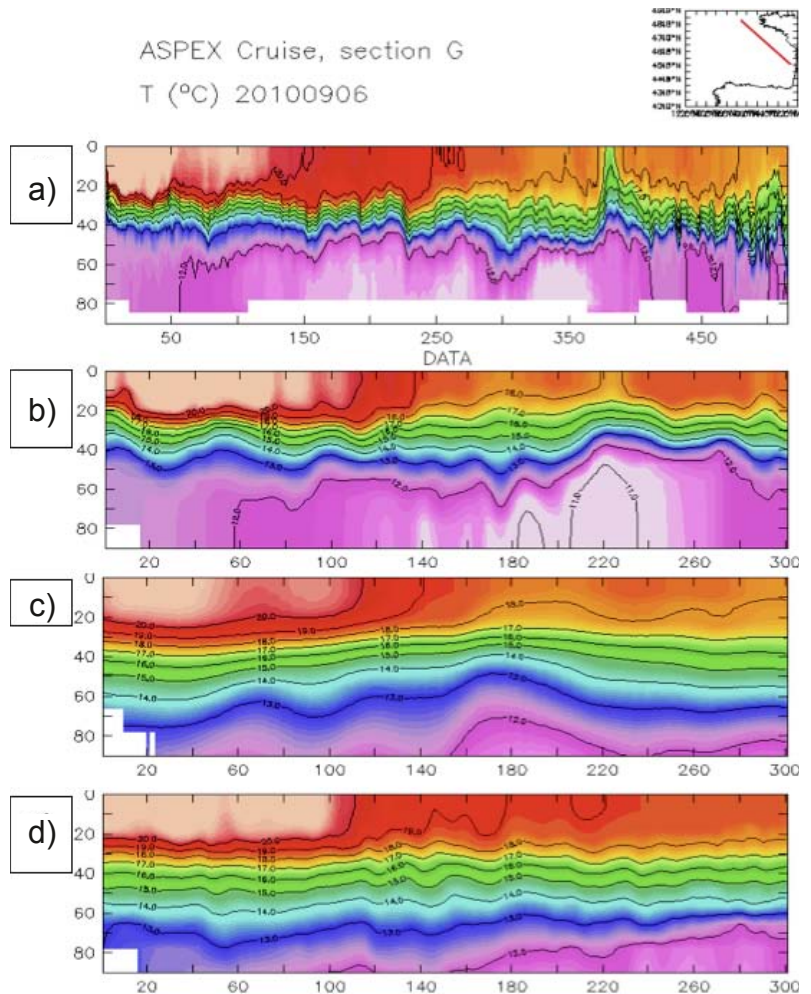


Figure 14:  
SLA comparison between  
a) IBI-REF,  
b) IBI-NUDG,  
c) PSY2 and  
d) AVISO.

In Fig. 15, the IBI-OPER, PSY2V4 and IBI-NUDG daily mean temperature of 2010-09-06 is compared to the ASPEX Cruise section one (Le Boyer et al, 2013), on the shelf in the Bay of Biscay off the Aquitaine and Britain French coasts. The thermocline as well as its associated temperature gradient is better resolved in IBI-NUDG with a depth between about 20m and 40m. The strongest observed eddies seem to be noticeable in the IBI-NUDG solution when the thermocline goes up for the anticlockwise eddies (cyclones) or down for the clockwise eddies (anticyclones). In this area, IBI-NUDG is free since the nudging from PSY2V4 is switched off above the shelf due to chosen tapering function. So the high frequency and small scale physical processes which are dominating in the shelf region, are better resolved by IBI-NUDG than PSY2V4 or IBI-OPER. Indeed, the physics, the resolution as well as the data used for the assimilation of PSY2V4 aren't adapted for this area, and the weekly restarting of IBI-OPER by PSY2V4 prevents small structures to develop on the shelf area.

Figure 15:  
Comparison of the temperature  
along the ASPEX Cruise  
section G (ASPEX campaign 2010, Louis  
Marié) on the 2010-09-06:  
a) observation,  
b) IBI-NUDG,  
c) PSY2,  
d) IBI-OPER.



## Downscaling from Oceanic Global Circulation Model towards Regional and Coastal Model using spectral nudging techniques: application to the Mediterranean Sea and IBI area models

In Fig. 16 the SST bias significantly decreases from *IBI-OPER* to *IBI-NUDG* on the shelf for the same reasons explained above. This decrease is particularly noticeable in the English Channel and the Ireland Sea where the strong tidal fronts prevail. A nudging in this area would be obviously useless since *PSY2V4* can't resolve tide processes.

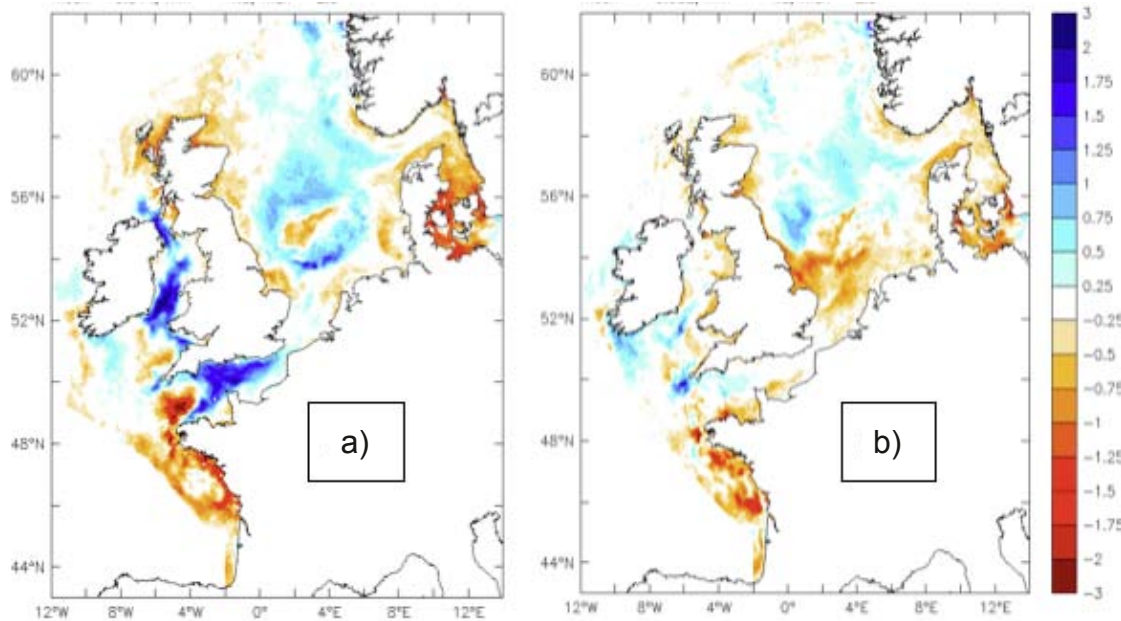


Figure 16: Mean SST bias vs CMS R/S data (Centre de Météo Spatial) in September 2010 (in °C):  
a) CMS - IBI-OPER , b) CMS - IBI-NUDG .

In Fig. 17 and 18 the SLA bias and RMS significantly decrease from *IBI-REF* to *IBI-NUDG* off the shelf. In this area, the large scale and low frequency process SLA is quite well represented by *PSY2V4* which assimilates altimetry data and consequently the spectral nudging improves *IBI* solution. These results complete the previous one (Fig. 16) and confirm the right choice of the tapering function which allows *IBI-NUDG* to run free in the shelf area.

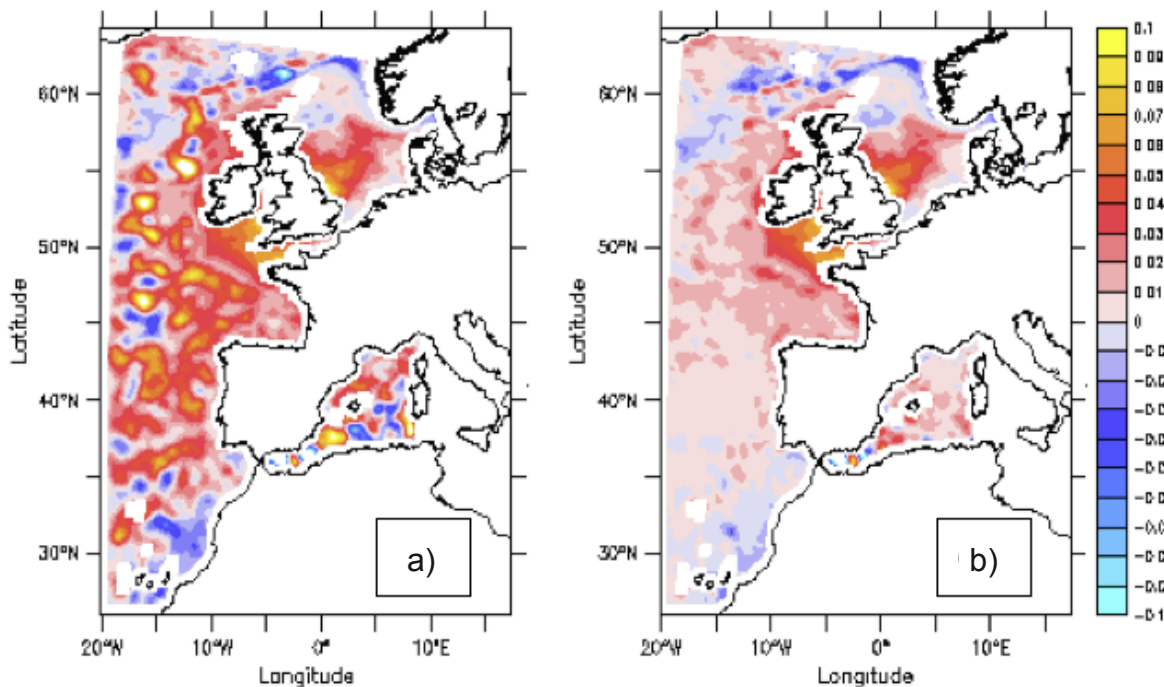


Figure 17: Mean SLA bias vs AVISO (in m) for the run period (2010/03/30 – 2010/10/18) :  
a) AVISO - IBI-REF , b) AVISO - IBI-NUDG .

Downscaling from Oceanic Global Circulation Model towards Regional and Coastal Model using spectral nudging techniques: application to the Mediterranean Sea and IBI area models

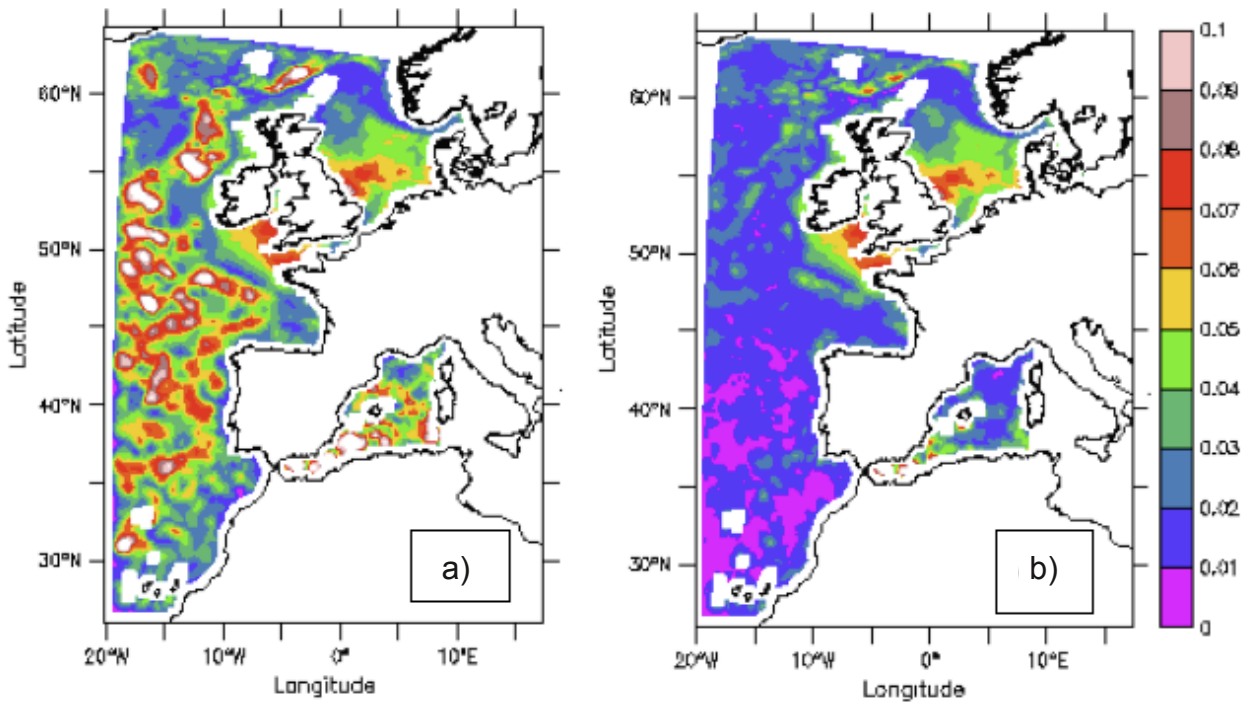


Figure 18: SLA RMS vs AVISO (in m) for the run period (2010/03/30 – 2010/10/18): a) AVISO - IBI-REF , b) AVISO - IBI-NUDG .

We can notice the bias and RMSE of IBI-NUDG seem to increase with the latitude off the shelf and especially along the shelf break. Indeed, the effective resolution of PSY2V4 decreases with the latitude and becomes too low in the high latitudes to resolve meso-scale structures: PSY2V4 is no more eddy-resolving. It can still represent large eddies advected in this area by the North Atlantic Drift (NAD) but not meso-scale eddies generated locally and especially close to the shelf break where slope current or other along break currents can become unstable.

Consequently an improvement of this spectral nudging method would consist in finding a low pass spatial filter depending on the latitude  $\varphi$  ; i.e. with a cut off frequency  $T_c(\varphi)$  increasing with  $\varphi$ . The energy injection scale described previously depends on the Rossby radius which is a characteristic scale of the meso-scale structures (Stammer 97, Penven et al 2005). If we consider in 1<sup>st</sup> approximation the first baroclinic Rossby radius  $R_0$  which decreases in the latitude  $\varphi$  : the higher is  $\varphi$  , the smaller is  $R_0$  and the larger is  $T_c$ . Chelton et al, 1998 generated a global climatology of  $R_0$  from T-S profiles and they established a least squares estimate of the zonally averaged  $R_0$  by regression onto a quadratic function of inverse latitude. As  $T_c$  must increase when  $R_0$  decreases, we can approximate  $T_c$  by a function of inverse of  $R_0$ . In low latitudes,  $R_0$  is large:  $R_0(0^\circ \leq |\varphi| \leq 10^\circ) = R_{0eq} \sim 200\text{km}$  on average according to the climatology of Chelton et al, 1998. If we suppose that the parent system resolution  $\Delta x$  is enough to resolve the large scale structures in the equatorial band, then we can consider  $T_c(0^\circ \leq |\varphi| \leq 10^\circ) = 1 \cdot \Delta x$ . So we can choose the following function:

$$T_c(\varphi) = R_{0eq} \cdot R_0^{-1}(\varphi) \cdot \Delta X \tag{5}$$

This function verifies the value of  $T_c \sim 7\Delta x$  in mid-latitudes as found in this study, with  $R_{0eq} \sim 200\text{km}$  and  $R_0(30^\circ \leq \varphi \leq 40^\circ) \sim 30\text{km}$ . The smoothing can be applied by band of latitude: each band ( $\varphi_0 \leq \varphi \leq \varphi_1$ ) can be defined by a specific integer  $T_c$  which is calculated by Eq. (5).

Mercator Ocean has developed a spectral nudging tool SPECI dedicated for the next IBI operational system version and possibly other regional systems embedded in global one. SPECI takes into account this improvement. Figure 19 sums up the steps of SPECI to generate the nudging fields.

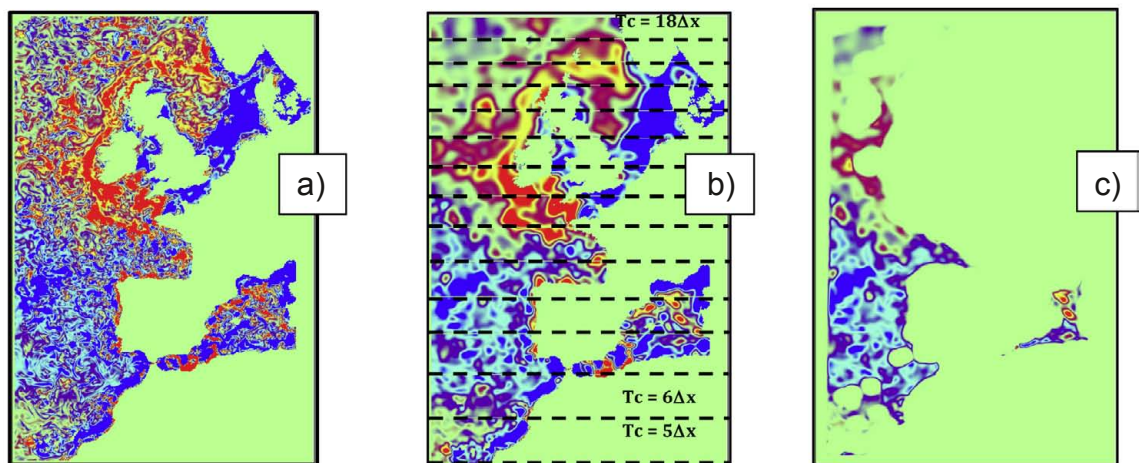


Figure 19: Steps of SPECI for the calculation of  $f(x,y,z) \cdot \langle X_p - X_c \rangle$ . SST is represented here. a) the difference of the weekly means of the SST of PSY2 and IBI, ie.  $X_p - X_c$ . b) the latitude-dependent space Shapiro smoothing of the previous difference, ie.  $\langle X_p - X_c \rangle$ . And c) the application of the tapering function, ie.  $f(x,y,z) \cdot \langle X_p - X_c \rangle$ .

## Downscaling from Oceanic Global Circulation Model towards Regional and Coastal Model using spectral nudging techniques: application to the Mediterranean Sea and IBI area models

### Conclusion - Perspectives

The spectral nudging technique appears as a promising method in order to maintain coherence between regional model and large scale analysis at least over a selected frequency and wavelength band (in this study: the scales  $> 50$  km and  $> 7$  days for the Med Sea case, and the scales  $> 45$  km and  $> 7$  days for the IBI case); it allows to take advantages from data assimilation performed at the global model while maintaining properly the smallest scales variability of the regional model.

Regarding the Med Sea model application, this result was highlighted by diagnostics made through comparisons with observations as satellite SST data which have shown that the bias with observations are reduced in the nudged simulation. The analysis of SSH spectrum over the domain in both simulations also showed that the energy associated to small scales are not significantly affected by the spectral nudging technique. Indeed, only the scales ranged in the frequency and wavelength band selected are nudged toward the global solution, leaving the regional smaller scales free to evolve.

Regarding the IBI model application, comparisons to SLA AVISO, SST CMS and ASPEX section have shown that the nudging has improved IBI model solution off the shelf area where IBI model can really take benefit of the assimilated solution of PSY2V4: the meso-scale eddies are better represented and located due to the SLA assimilation in PSY2V4 among other. Compared to the present operational IBI model (IBI-OPER) which is weekly restarted by PSY2V4 in the whole domain, the SST bias strongly decreases on the shelf where the IBI nudged model (IBI-NUDG) is let free. Indeed, the solution of the high frequency and high resolution IBI model is best on the shelf where data assimilated in PSY2V4 are poor and the resolution of the large model isn't enough. This result is confirmed through the comparison with the ASPEX section on the shelf: the thermocline characteristics of free solution of IBI-NUDG model are far more realistic than PSY2V4 or IBI-OPER.

In addition spectral nudging technique is a low computer cost technique, not intrusive in the code and easy to manage in an operational chain. In this context, the introduction of spectral nudging technique could improve the operational scheme providing an alternative to frequent re-initialisation of the regional model. Besides, spectral nudging could be also a very efficient method useful for regional downscaling of the climate change scenarios.

In terms of perspectives, IBI system nudged by PSY2V4 (and then PSY4) is planned at the end of MyOcean2 first as a demo system and then as a fully operational system for MyOcean Follow On. This update will be applied by Puertos del Estado in the nominal MyOcean IBI system by using a tool SPECI (SPECtral nudging tool) developed by Mercator Ocean. This tool is easy to set up and parameterize, and it generalizes the method applied in the IBI case in this paper since it allows the low pass spatial filter to depend on the latitude.

MANGA system (MANche GAscogne coastal system of PREVIMER) nudged by IBI one is planned too: firstly in reanalysis mode for a 10-year simulation between MANGA and IBIRYS (IBI reanalysis) in the framework of the PPR ENIGME (Evolution Interannuelle de la dynamique dans le golfe de Gascogne et la Manche) lead by IFREMER, and secondly in operational mode. Thus, the downscaling from the large scale global and regional EU systems to the national coastal system will become a reality.

## Downscaling from Oceanic Global Circulation Model towards Regional and Coastal Model using spectral nudging techniques: application to the Mediterranean Sea and IBI area models

### References

- Alexandru, A., R. de Elía, R. Laprise, L. Separovic, and S. Biner, 2009: Sensitivity Study of Regional Climate Model Simulations to Large-scale Nudging Parameters. *Mon. Wea. Rev.*, 137,1666–1686
- Bloom, S. C., Takacs, L. L., Da Silva, A. M. and Ledvina, D., 1996: Data assimilation using incremental analysis updates. *Mon. Wea. Rev.*,124, 1256-1271.
- Cailleau, S., J. Chanut, J.-M. Lellouche, B. Levier, C. Maraldi, G. Reffray, M. G. Sotillo 2012: Towards a regional ocean forecasting system for the IBI (Iberia-Biscay-Ireland area): developments and improvements within the ECOOP project framework. *Ocean Sci.*, 8, 143-159.
- Chelton, D. B., A. R DeSzoeke, M. G. Schlax, 1998: Geophysical variability of the first baroclinic Rossby radius of deformation. *J. Phys. Oceanogr.*, 28, 433-460.
- Eden, C., R. J. Greatbatch, and C. W. Böning, 2004: Adiabatically correcting an eddy-permitting model using large-scale hydrographic data: Application to the Gulf Stream and the North Atlantic Current. *J. Phys. Oceanogr.*, 34, 701– 719.
- Klein, P., Hua, B., Lapeyre, G., Capet, X., Gentil, S. L., Sasaki, H., 2008 : Upper ocean turbulence from high 3-D resolution simulations, *J. Phys Oceanogr.* **38**, 8 1748-1763.
- Lascaratos, A., R. Williams, and E. Tragou, 1993: A mixed layer study of the formation of Levantine Intermediate Water *J. Geo-phys. Res.*, 98 (C8), 14 739–14 749.
- Lazure P., Dumas, F., 2008: An external-internal mode coupling for a 3D hydrodynamical model for applicaitons at regional scales (MARS). *Adv. In. Water Resour.* 31(12): 233-250.
- Le Boyer, A., G. Charria, B. Le Cann, P. Lazure, L. Marié, 2013: Circulation on the shelf and the upper slope of the Bay of Biscay. *Continental Shelf Research*, 55, 97-107.
- Madec G., Delecluse P., Imbard M., Lévy C., 1998: OPA 8.1 Ocean general circulation model reference manual. Institut Pierre-Simon Laplace, 20, p. 91.
- Madec G., 2008: NEMO Ocean General Circulation Model Reference Manuel. Internal Report. LODYC/IPSL, Paris.
- Maraldi C., J. Chanut, B. Levier, N. Ayoub, P. De Mey, G. Reffray, F. Lyard, S. Cailleau, M. Drevillon, E. A. Fanjul, M. G. Sotillo, P. Marsaleix, and the Mercator Research and Development Team .NEMO on the shelf: assessment of the Iberia–Biscay–Ireland configuration. *Ocean Sci.*, 9, 745–771, 2013.
- MEDOC Group, 1970: Observation of formation of deep water in the Mediterranean Sea, 1969. *Nature*, 227:1037-1040.
- Millot, C., 1987: Circulation in the Western Mediterranean. *Oceanol. Acta* 10 2, 143–149.
- Millot C., 1990: The Gulf of Lions' hydrodynamics. *Continental Shelf Research*, 10 (9-11) : 885-894.
- Millot C., 1999: Circulation in the Western Mediterranean Sea. *Journal of Marine Systems*, 20 : 423-442.
- Penven, P and V. Echevin, 2005: Average circulation, seasonal cycle, and mesoscale dynamics of the Peru Current System: a modeling approach. *J. Geophys. Res.*, 110 (C1), 1-21.
- Sheng, J., Greatbatch, R.J., Tang, L., Zhai, X., 2005: A new two-way nesting technique for ocean modeling based on the smoothed semi-prognostic method. *Ocean Dynamic*, 55, 62-17.
- Skamarock, W. C., 2004: Evaluating Mesoscale NWP Models Using Kinetic Energy Spectra. *Mon. Wea., Rev.*, 132, 3019-3032
- Stammer, D., 1997: Global characteristics of ocean variability estimated from regional TOPEX/Poseidon altimeter measurements. *J. Phys. Oceanogr.*, 27, 1743–1769.
- Von Storch, H., H. Langenberg, and F. Feser, 2000: A spectral nudging technique for dynamical downscaling purposes. *Mon. Wea. Rev.*, 128, 3664–3673.
- Wüst, G., 1961: On the vertical circulation of the Mediterranean Sea. *J. Geophys. Res.*, 66, 3261–3271